Chinese Journal of
POLYMER SCIENCE

RESEARCH ARTICLE

https://doi.org/10.1007/s10118-026-3643-4
Chinese J. Polym. Sci.

Processing-integrated Machine Learning Models for Predicting and Optimizing Mechanical Properties of Polyimides

Wei-Long Hu[a,b], Hao-Ke Qiu[a,b], En-Zhe Jing[a,b], Wan-Chen Zhao[b], Hai-Yang Huo[b], and Zhao-Yan Sun[a,b,c*]

[a] *School of Applied Chemistry and Engineering, University of Science and Technology of China, Hefei 230026, China*
[b] *State Key Laboratory of Polymer Physics and Chemistry & Key Laboratory of Polymer Science and Technology, Changchun Institute of Applied Chemistry, Chinese Academy of Sciences, Changchun 130022, China*
[c] *Jilin Provincial International Cooperation Key Laboratory for Polymer Processing Physics, Changchun 130022, China*

Electronic Supplementary Information

Abstract Polyimides (PIs) are widely used in industry owing to their excellent mechanical properties and thermomechanical stability, which depend not only on molecular structure but also on processing conditions. In this study, we present a machine-learning-based strategy for predicting and optimizing the mechanical properties of PI materials by explicitly incorporating processing information into predictive models. Three machine learning models were developed to evaluate PI structures together with thermal imidization parameters, with the aim of improving the prediction accuracy of mechanical properties and enhancing the interpretability of structure-processing-property relationships. By analyzing structural and processing descriptors, key factors influencing tensile strength, Young's modulus, and elongation at break were identified. The results indicate that, in addition to molecular descriptors, processing-related features plays a substantial role on multiple mechanical properties. Based on the trained models, we further developed an automated tool that accepts a SMILES representation of a PI structure as input and outputs the predicted mechanical properties along with the corresponding processing conditions associated with optimal performance. This work provides a data-driven framework for guiding PI material design and process optimization, and offers a practical basis for future experimental validation. Our proposed approach is readily extendable to other polymer systems and polymer composites where processing plays an important role in determining mechanical behavior.

Keywords Explainable machine learning; Polyimides; Mechanical property

Citation: Hu, W. L.; Qiu, H. K.; Jing, E. Z.; Zhao, W. C.; Huo, H. Y.; Sun, Z. Y. Processing-integrated machine learning models for predicting and optimizing mechanical properties of polyimides. *Chinese J. Polym. Sci.* https://doi.org/10.1007/s10118-026-3643-4

INTRODUCTION

Polyimides (PIs) are a class of high-performance polymers widely used in aerospace, electronics, and energy-related applications owing to their excellent mechanical strength, thermal stability, and chemical resistance.[1–13] In these applications, mechanical properties, such as elongation at break (ε), tensile strength (σ), and Young's modulus (E), are critical for ensuring structural reliability and long-term service performance.

In practical synthesis and processing, however, the mechanical behavior of PI materials is not determined solely by molecular structure. Variations in processing conditions, particularly thermal imidization temperature and heating duration, often lead to substantial differences in mechanical performance even for PIs with identical chemical backbones.[14–17] These processing-dependent effects influence chain packing, degree of imidization, residual stress evolution, and interfacial interactions, making mechanical properties highly sensitive to processing history. As a result, predicting PI mechanical performance remains a challenging task from both experimental and modeling perspectives.

Machine learning (ML) has emerged as an effective tool for modeling polymer properties and accelerating materials design, and a growing number of ML-based studies have been reported for PI systems.[18–31] For example, ML-based quantitative structure-property relationship (QSPR) models have been successfully developed to predict the glass transition temperature (T_g) of PIs,[32,33] and graph-based models have been applied to capture thermal and dielectric behaviors in PI homopolymers and composites.[34–36]

Despite this progress, accurately modeling the mechanical properties of PI materials remains challenging. Recent ML efforts targeting polymer and PI mechanical performance have largely relied on intrinsic molecular descriptors and structural representations.[37–41] Even when advanced learning architectures are employed, the prediction accuracy for mechanical properties is often limited, as demonstrated in recent PI-focused mechanical ML studies, including our own work.[42] A primary reason for this limitation is that mechanical properties are not intrinsic material constants but are strongly mod-

* Corresponding author, E-mail: zysun@ciac.ac.cn
Received February 3, 2026; Accepted March 5, 2026; Published online April 16, 2026

ulated by processing history, which is rarely incorporated explicitly into existing ML models.[14–16] As a result, a gap persists between ML predictions and experimental observations, particularly when models are used to guide processing-sensitive mechanical optimization.

To address this challenge, the present work develops a machine-learning framework for predicting the mechanical properties of PI materials by explicitly integrating processing parameters associated with thermal imidization into the model. A dataset comprising PI molecular structures, processing conditions, and corresponding mechanical properties was constructed, including ε, σ, and E. By analyzing molecular and processing descriptors, we investigate the factors governing mechanical performance and demonstrate how incorporating processing information improves model performance. Furthermore, the developed framework is integrated into an automated tool which can predict mechanical properties and associated processing conditions directly from a SMILES representation of a PI structure, providing a practical strategy for data-driven design and process optimization of PI materials. Our approach can also be easily extendable to other polymer systems and polymer nanocomposites.[43]

MATERIALS AND METHODS

The overall workflow of this study is illustrated in Fig. 1. We first collected PI material data from various literature sources, focusing on three key mechanical properties: ε, σ, and E. Based on these data, we constructed a dataset that includes SMILES representations of PI structures, processing information describing the thermal imidization conditions, and the corresponding mechanical properties. We then employed multiple machine-learning models to predict the mechanical properties and selected the models with the best predictive performance. To assess feature importance, we applied SHapley Additive exPlanations (SHAP) analysis, allowing us to identify the key factors influencing each mechanical property. In addition, we investigated the relationships between the processing descriptors and mechanical performance, illustrating how different aspects of the thermal imidization process contribute to the observed material properties. Finally, we used the trained ML models to develop an automated tool capable of optimizing the processing descriptors directly from an input SMILES string, yielding both the predicted optimal mechanical properties and the corresponding five-dimensional processing-feature vector.

Data Collection

We manually extracted 307 data points from the literature and collected detailed information for each entry, including the SMILES structure,[44–48] stepwise temperature and duration profiles from the thermal imidization process, and the corresponding mechanical properties ε, σ, and E. Details of our data sources can be found in the Table S1 (in the electronic supplementary information, ESI). It is worth mentioning that during the data collection process, we found that different types of PI materials

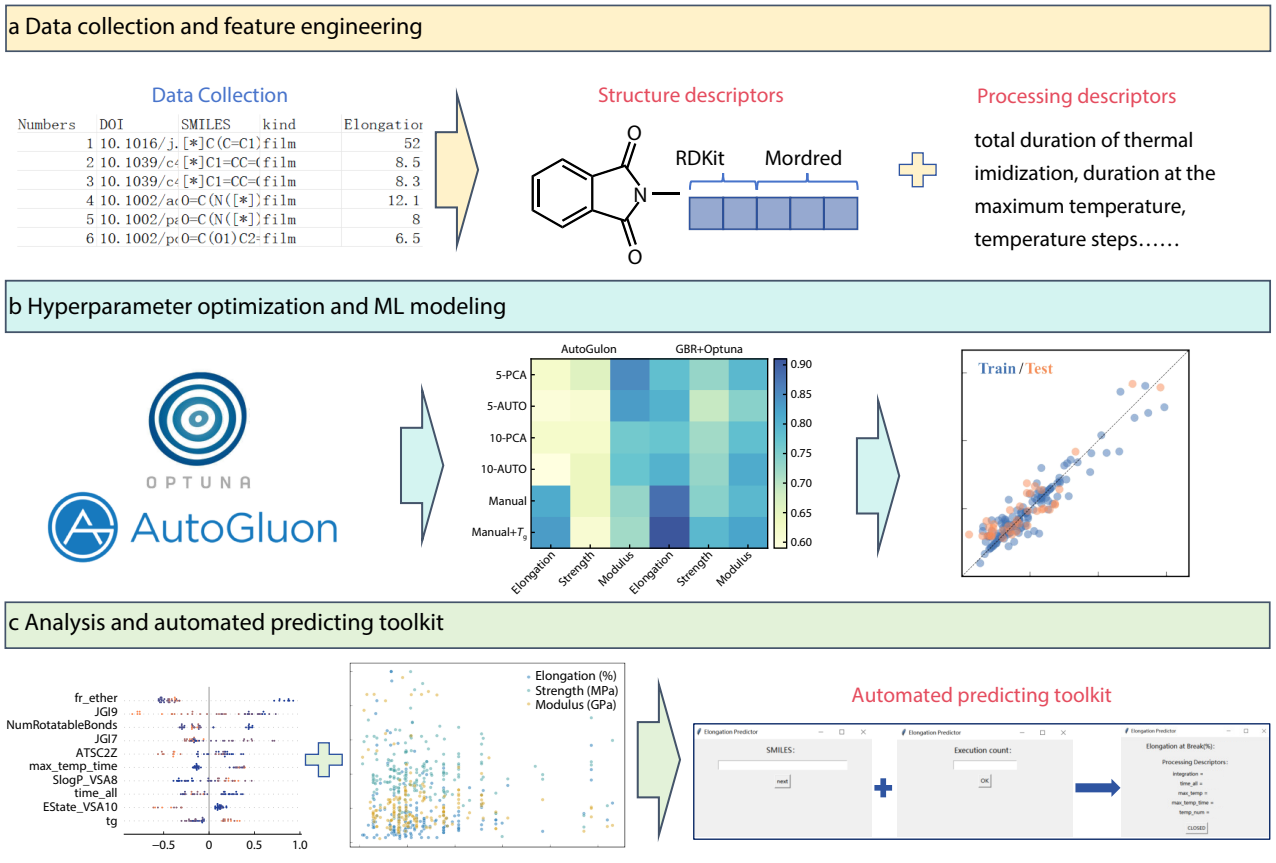

Fig. 1 Workflow used in this work. (a) Data collection and feature engineering; (b) ML modeling and feature importance; (c) Analysis on the structure and processing information, and automated predicting toolkit.

often have significant differences in mechanical properties. To ensure the accuracy of our research, the data points we selected in this work were all film PI materials. To illustrate the structural diversity of the PI materials in our dataset, we visualized their chemical space using t-SNE in Fig. S1 (in ESI). We use RDKit and Mordred toolkits to calculate 1813 descriptors of each SMILES structure, and then use Lsig strategy[49] to filter these descriptors before t-SNE visualization to minimize redundant induced bias. The results show a broad distribution of molecular structures, supporting the representativeness of our dataset. In addition, the distributions of three mechanical properties were normalized, and Fig. S2 (in ESI) shows that the normalized values approximate a Gaussian distribution, indicating that the dataset is well suited for predictive modeling.

To further investigate the relationships among the mechanical properties, we visualized the pairwise distributions of the PI dataset in Fig. S3 (in ESI). The results reveal no significant correlations among the three properties, suggesting the presence of complex nonlinear interactions.

Molecular Feature Engineering

During the selection of SMILES-related molecular descriptors, we initially obtained 1813 valid descriptors from two widely used cheminformatics toolkits, RDKit and Mordred. After the simplest variance screening, 956 descriptors remained for further analysis. We grouped these features into four categories based on their physicochemical meaning-structural, electronic, topological, and hybrid descriptors. We then employed the AutoGluon automated framework to construct models using our dataset and to perform automated hyperparameter optimization. AutoGluon evaluates multiple algorithms and generates feature-importance rankings for each model. AutoGluon also produces an ensemble model by aggregating all base learners, usually achieving a high R^2 value. However, due to its lack of interpretability, we did not use this ensemble model for further analysis, but only selected the top 10 highest-ranking descriptors from the ensemble model. In order not to miss those descriptors which may be relative to the polymer structure-property relationships, we supplemented the descriptor set by adding additional features that frequently appeared across different models to ensure comprehensive structural representation. Details are provided in https://github.com/Weilong-Hu/PI Processing/molecular features supplement.

Subsequently, we calculated the Spearman coefficients between each performance and feature to demonstrate the correlation between features and performance. We found that most of the coefficients are about 0.3, which is sufficient to indicate the correlation between features and performance. Meanwhile, we provide the Spearman coefficients between each mechanical property and the selected features in Table S12 (in ESI).

Processing Feature Engineering

We incorporated thermal imidization processes as the processing-related information in our dataset. All processing data were first converted into temperature-time gradient maps, from which we extracted descriptors using two approaches: convolutional neural networks (CNNs) and manually engineered features. For the CNN-based approach, we applied two dimensionality-reduction methods (principal component analysis (PCA) and autoencoders) combined with two target dimensionalities (5 and 10). This resulted in four distinct feature-representation schemes. For the manually engineered features, we selected five descriptors: integration (the integral of the temperature-time profile), time_all (total duration of thermal imidization), max_temp (maximum temperature reached), max_temp_time (duration at the maximum temperature), and temp_num (the number of temperature steps during the imidization process). We take a temperature-time gradient plot as an example and show the specific meanings of the 5 features we manually extracted in Fig. 2. Furthermore, because the T_g of PI structures may be mechanistically linked to mechanical properties through structure-property relationships, we also considered the inclusion or exclusion of T_g as a variable when constructing the manually extracted processing descriptors.

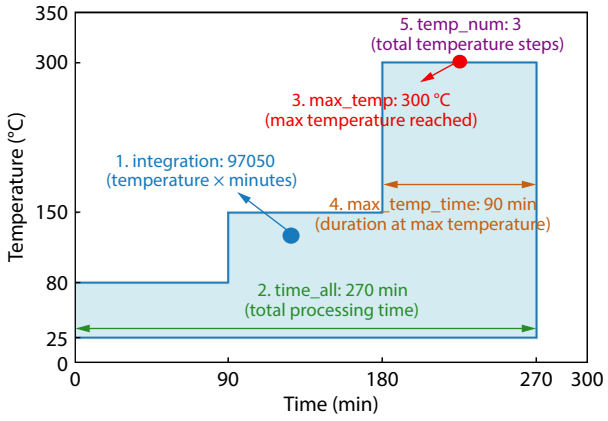

Fig. 2 The specific meanings of 5 features in the temperature-time processing map.

Hyperparameter Optimization and Model Building

We employed two approaches for model construction and hyperparameter optimization: AutoGluon (for automated model generation and hyperparameter tuning) and GBR+Optuna[50] (using a Gradient Boosting Regressor coupled with Optuna-based optimization). For each of the six processing-feature representations, we concatenated the processing descriptors with the selected molecular descriptors and subsequently built ML models using both approaches. Model performance was evaluated based on the coefficient of determination (R^2). For AutoGluon we selected, the best-performing model among the multiple base learners was generated for each mechanical property. A heatmap summarizing the model comparison results is provided in Fig. 3.

We found that the GBR+Optuna models generally outperformed those generated by AutoGluon. In addition, processing features obtained through manual extraction consistently led to better model performance than those derived from convolutional neural networks. We attribute this improvement to the fact that the manually engineered descriptors preserve the underlying physical meaning of the thermal imidization process and simultaneously enhance model interpretability. Furthermore, after incorporating T_g as an additional descriptor, the GBR+Optuna models exhibited a modest performance gain. Detailed numerical results for all models are provided in Table S2 (in ESI). In this process, we divided the dataset into training and testing sets (8:2 ratio and random_seed = 42) and for each property the molecular descrip-

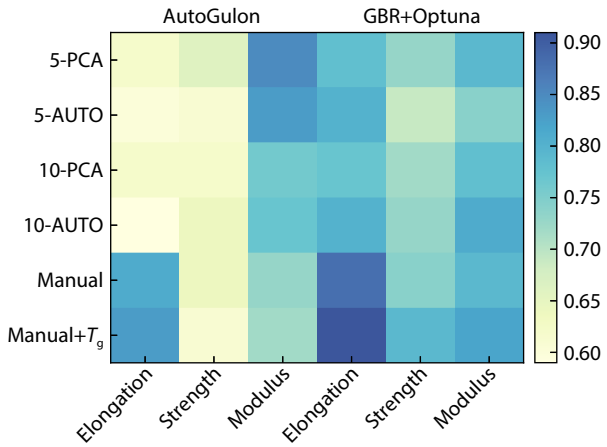

Fig. 3 Model performance comparisons across different optimization stages and feature acquisition methods.

tors used to describe SMILES are the same, in which only the processing descriptors are changed. We provide detailed information of processing descriptors in Table S6 (in ESI) and the names of molecular descriptors we used in Table S7 (in ESI).

After completing the model construction, we further developed an automated tool based on our optimized models. This tool accepts a SMILES string and a user-defined number of optimization iterations as input, and then performs Bayesian optimization on the processing descriptors with the goal of maximizing the predicted mechanical performance. The detailed workflow is illustrated in Fig. 4. Upon completion of the specified number of optimization cycles, the program outputs both the best predicted mechanical property of the given structure and the corresponding set of processing descriptors required to achieve it. Taking the elongation at break as an example, we used this automated tool to optimize the performance of an existing structure in a dataset. We found that the optimized process parameters with better performance were in line with our physical knowledge, which verifies the reliability of our automated tool. The comparison of the results before and after optimization are shown in Table S10 (in ESI). This functionality provides practical guidance for designing more rational thermal-imidization processes, thereby shortening the development cycle of new PI materials. For detailed code and files, please see https://github.com/Weilong-Hu/PI Processing/prediction.

RESULTS AND DISCUSSION

Model Training Results

We evaluated the performance of our machine-learning models on both the training and testing subsets of the dataset, as illustrated in Fig. 5. Blue and red markers correspond to the predicted values for the training and test sets, respectively. To assess model performance, we calculated the coefficient of determination (R^2), mean absolute error (MAE), mean squared error (MSE), root-mean-square error (RMSE), and mean absolute percentage error (MAPE) for the test sets. The detailed numerical results of these metrics are provided in Table S3 (in ESI). In addition, Table S4 (in ESI) includes comprehensive information on all three final models, including computational facility, training time, prediction speed, and hyperparameters, offering additional dimensions for evaluating model performance.

Compared with our previous work in which ML models were constructed using only molecular descriptors of PI homopolymers,[42] we found that the present models exhibit consistently high prediction accuracy of mechanical properties. The specific performance of the models in both scenarios is detailed in Table S9 (in ESI). This indicates that incorporating processing information indeed exerts a positive influ-

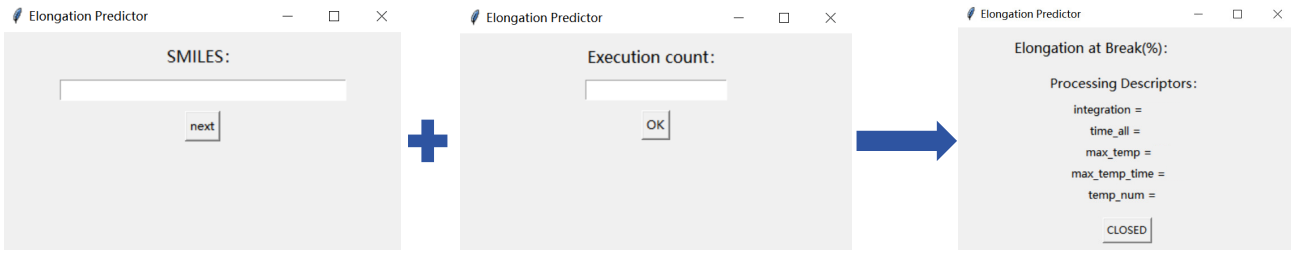

Fig. 4 Workflow used in our automated tool.

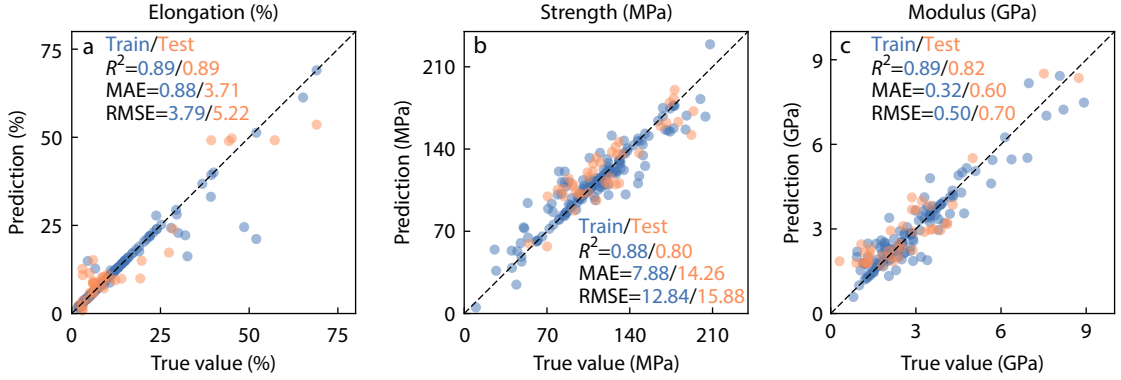

Fig. 5 Predictive performance of the best model for each mechanical property: (a) ε using the GBR; (b) σ using the GBR; (c) E using the GBR.

ence on model performance. Meanwhile, we observed a pronounced improvement in prediction accuracy for ε and E, suggesting that processing conditions have a more substantial impact on the rigidity of PI materials. This can be attributed to the fact that, in practical mechanical testing, failure of PI materials typically arises from interchain slippage rather than chain scission.

SHAP Analysis

We observed that several processing-related features consistently appear among the most influential descriptors in the SHAP plots for all three mechanical properties, as shown in Fig. 6. This indicates the importance of processing conditions in determining the mechanical performance of PI materials. Detailed explanations of the processing descriptors are provided in the Table S5 (in ESI). Interestingly, the descriptor time_all, which represents the total heating duration, appears prominently across all three properties. This is probably due to the fact that the overall heating time may strongly affect the degree of imidization. Insufficient heating leads to incomplete imidization, whereas excessively long heating may alter chain entanglement or introduce local defects. In addition, the descriptors integration, which reflects the overall heating-gradient profile, and max_temp_time, which denotes the duration at the maximum temperature, also appear frequently among the key contributors for the three mechanical properties. This highlights the significance of heating duration in the underlying thermochemical processes governing PI mechanical behavior.

For the molecular descriptors, we categorized the features collected from RDKit and Mordred into four groups based on structural, electronic, topological, and hybrid descriptors. Detailed explanations of these structural features are provided in https://github.com/Weilong-Hu/PI Processing/molecular features meanings. We found that, across all three mechanical properties, descriptors associated with electronic and topological characteristics appear most frequently, indicating that the mechanical behavior of PI materials is strongly influenced by electronic distribution and molecular topology. For ε in Fig. 6(a), the most influential descriptor is GGI8, which captures heavy-atom contributions at the 8th-order topological distance. This suggests that the spatial distribution of heavy atoms and their interactions with surrounding atoms play a key role in determining the flexibility of PI materials. Moreover, the JGI series-descriptors frequently appear, which represent atom-level properties across various topological distances. This further reinforces the importance of topological information in governing material flexibility. For σ in Fig. 6(b), the most critical descriptor identified is AETA_beta_ns, which relates to the sigma-electron contribution of valence electrons. Its related descriptor AETA_beta also appears prominently. Among the four categories, electronic descriptors occur most frequently for σ, demonstrating the strong correlation between σ and electronic distribution. This indicates a coupling between σ of polymer and atomic-level electronic interactions. For E in Fig. 6(c), the repeated appearance of JGI descriptors again highlights the intrinsic relationship between ε, which represents flexibility, and E, which represents rigidity. This also suggests that certain descriptors influence multiple mechanical properties simultaneously by capturing intrinsic topological characteristics of PI materials. The definitions and categories of all descriptors shown in the Fig. 6 are provided in Table S11 (in ESI).

Influence of Processing Features on Mechanical Properties of PI

After normalizing the five processing descriptors and the three

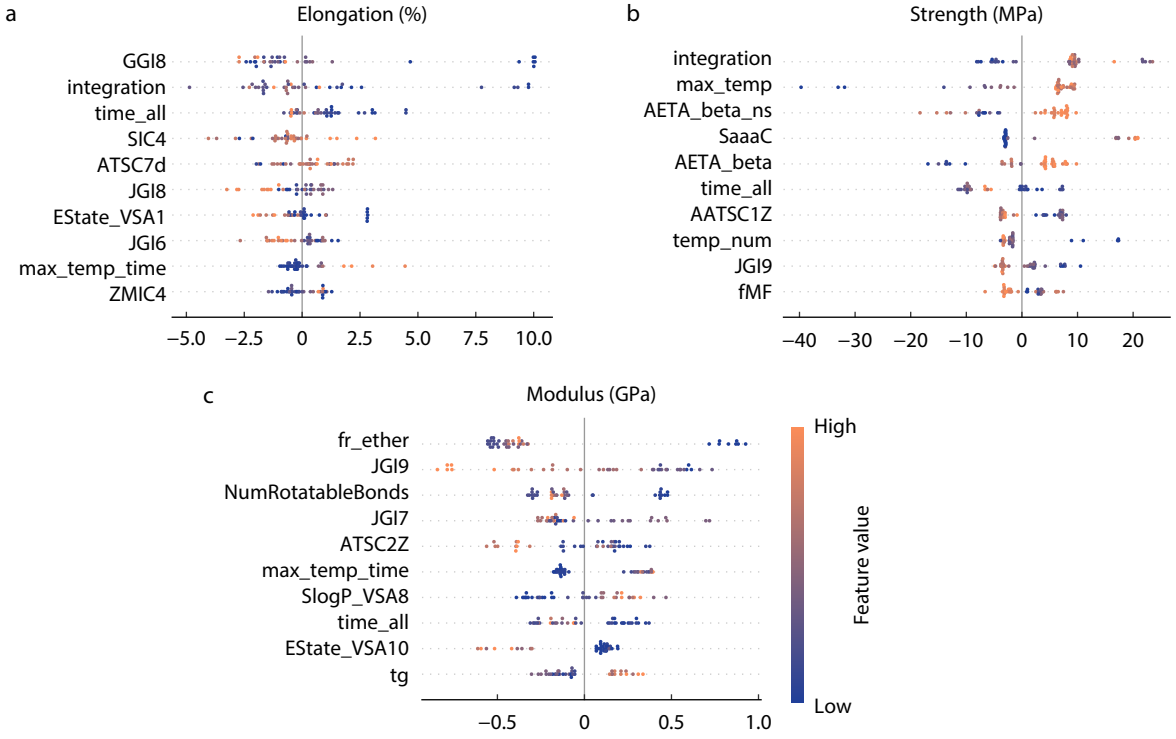

Fig. 6 Feature importance analysis of the best model showing (a) SHAP values for ε, (b) SHAP values for σ, and (c) SHAP values for E.

https://doi.org/10.1007/s10118-026-3643-4

mechanical-property datasets in Fig. 7, we compared the influence of each processing feature on different mechanical properties. Consistent with the SHAP analysis, the descriptor time_all (total duration of the thermal imidization process) exerts a pronounced influence on all three mechanical properties. Similarly, max_temp_time (duration at the maximum temperature) plays an important role in multiple mechanically correlated properties. As shown in Fig. 7(d), data points corresponding to both high ε and long heating time are largely absent. This result aligns with the SHAP result that time_all generally contributes

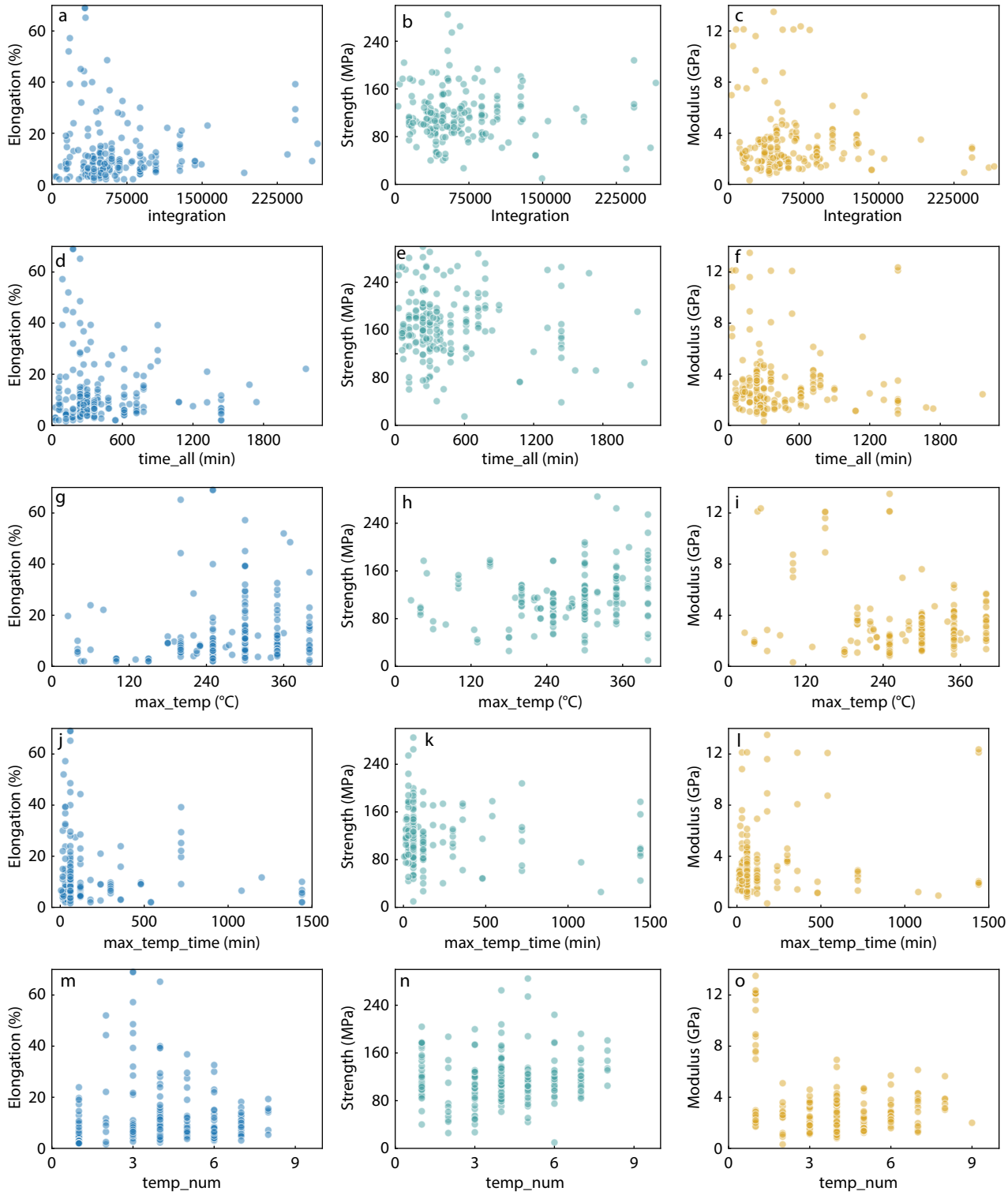

Fig. 7 Scatter plots of the relationship between various processing features and the three mechanical properties including elongation at break (a, d, g, j, m), tensile strength (b, e, h, k, n), and modulus (c, f, i, l, o).

https://doi.org/10.1007/s10118-026-3643-4

negatively to ε. This is resulted from the fact that prolonged heating may disrupt the originally stable intermolecular interactions, thereby facilitating chain slippage or other molecular motions that reduce ε. Note that some descriptors show upper boundary properties (such as max_temp in Fig. 7g and temp_num in Fig. 7m). This indicates that there may exist some optimum processing parameters during thermal imidization. For max_temp_time, we observed that most blue points representing E lie on the left side of Fig. 7(l), indicating shorter durations at the maximum temperature. However, a small number of samples exhibit high E even under long-duration heating. By tracing these samples, we found that they were processed at relatively low maximum temperatures, corresponding to long-term imidization at lower thermal stress. This implies that at high temperatures and rapid heating, structural defects are more likely to form within the material. In contrast, long-duration imidization at lower temperatures results in less damage to polymer chains during dehydration and may have a more stable internal structure.

At the same time, we noticed that the distribution of data points in Fig. 7 is mostly scattered and lacks clear patterns, which is probably due to the presence of multiple PI structures and process information in our dataset. To illustrate the processing effect on the mechanical properties of PI, we selected a PI structure with the most process information from the dataset and analyzed it separately in order to obtain more obvious physical insights, as is shown in Fig. 8. In addition, we presented the numerical values of the processing descriptors of data points with the best elongation, strength and modulus in Table S8 (in ESI).

In Fig. 8, ε decreases when either the thermal treatment temperature is excessively high or the treatment duration is prolonged. Processes exhibiting higher ε (Figs. 8b, 8c, 8h and 8i) are generally characterized by relatively low treatment temperatures. In contrast, Fig. 8(j) suggests that under high-temperature conditions, an extremely short reaction time may also contribute to improved ε. This indicates that lower processing temperatures lead to incomplete imination, thereby increasing chain mobility and facilitating chain stretching during deformation.

For σ, the maximum value is observed for the process shown in Fig. 8(e). Moreover, as presented in Figs. 8(e), 8(g), 8(k) and 8(l), processes with higher σ are predominantly associated with elevated thermal treatment temperatures. This suggests that higher processing temperatures promote chain crosslinking, which will strengthen intermolecular interactions and enhance σ.

E shows a trend similar to that of σ. Processes with higher E (>2 GPa), as illustrated in Figs. 8(e), 8(g), 8(k) and 8(l), generally involve higher maximum treatment temperatures (≥ 300 °C). These results indicate that the thermal imidization process affects multiple correlated mechanical properties through its influence on chain packing, cross-linking and structural organization.

Interestingly, processes that yield higher σ and E are often associated with more complex heating profiles involving multiple temperature gradients, while their ε is generally lower. This behavior is likely related to the degree of annealing during thermal imidization. A multistep heating profile can suppress excessive solvent evaporation at early stages, thereby reducing the formation of localized defect structures. At intermediate temperature ranges, limited chain mobility allows for conformational adjustment and chain rearrangement, whereas at higher temperatures the system becomes fixed in a denser structural state. This evolution enhances the stiffness and σ of the material but simultaneously increases its brittleness.

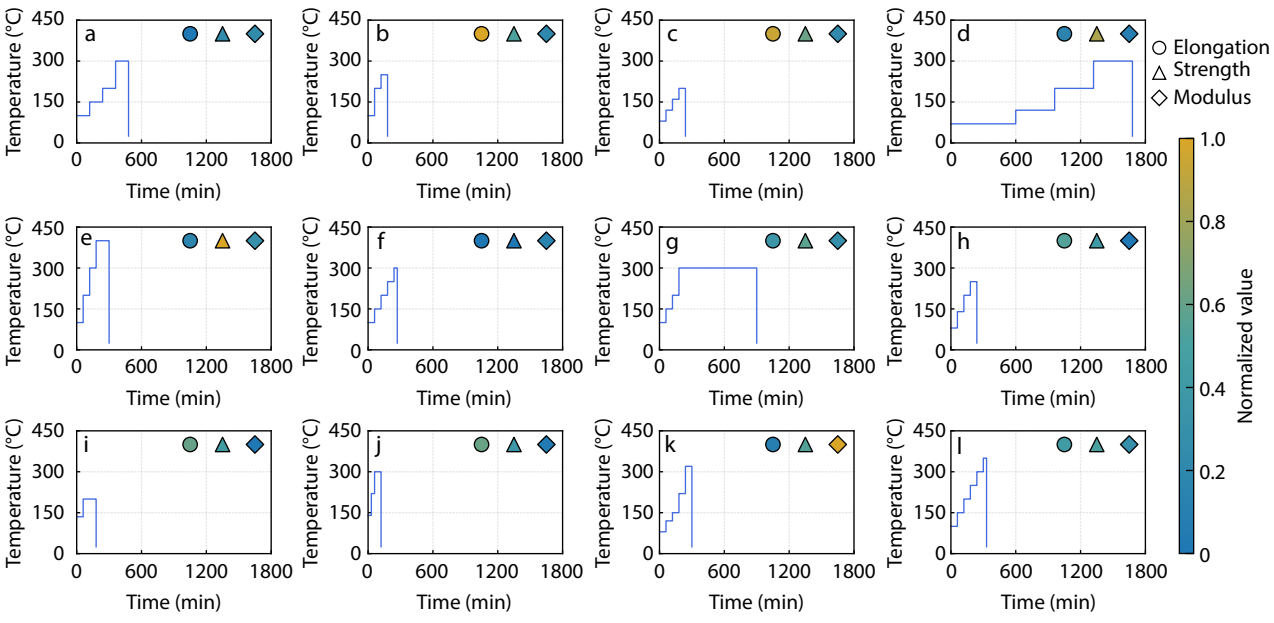

Fig. 8 Twelve collected processing curves (a–l) for a typical PI structure. The three symbols in the top right corner of each subfigure represent the elongation at break (circle), tensile strength (triangle), and modulus (diamond), respectively, where the colors of symbols indicate the re-scaled value of each mechanical property.

https://doi.org/10.1007/s10118-026-3643-4

CONCLUSIONS

In this study, we developed a machine-learning-based strategy for predicting and optimizing the mechanical properties of polyimide materials by considering molecular structure and processing information. Three predictive models were constructed to evaluate PI structures in combination with thermal imidization parameters, and an automated workflow was established to identify processing conditions associated with favorable mechanical performance directly from an input SMILES string.

The results demonstrate that, in addition to molecular descriptors, processing-related features exert a substantial influence on PI mechanical behavior. In particular, descriptors associated with heating duration consistently contribute to elongation at break, tensile strength, and Young's modulus, suggesting that thermal imidization history plays an important role in modulating chain packing and intermolecular interactions. These findings provide a data-driven perspective on the variability of mechanical properties observed in experimentally synthesized PI materials.

Although the present study focuses on PI systems, the proposed framework is general and can be extended to other polymers and polymer composites, provided that sufficient processing and property data are available. The lack of direct experimental validation remains a limitation of this work, but all models and tools have been made publicly accessible to facilitate future experimental verification. Continued expansion of the dataset and integration of experimental feedback will further improve the reliability and applicability of the proposed approach.

Conflict of Interests

The authors declare no interest conflict.

Electronic Supplementary Information

Electronic supplementary information (ESI) is available free of charge in the online version of this article at http://doi.org/10.1007/s10118-026-3643-4.

Data Availability Statement

The data that support the findings of this study are available from the corresponding author upon reasonable request. The author's contact information: zysun@ciac.ac.cn (Z.Y.S.)

ACKNOWLEDGMENTS

This work was financially supported by the National Natural Science Foundation of China (No. 52293471) and the Jilin Provincial Science and Technology Development Program (Nos. SKL202602006JC, SKL202502004JC). We are also grateful for the essential support of Jilin Provincial International Cooperation Key Laboratory for Polymer Processing Physics and the Network and Computing Center, Changchun Institute of Applied Chemistry, Chinese Academy of Sciences.

REFERENCES

1 Plis, E. A.; Engelhart, D. P.; Cooper, R.; Johnston, W. R.; Ferguson, D.; Hoffmann, R. Review of radiation-induced effects in polyimide. *App. Sci.* **2019**, *9*, 1999.
2 Wu, X.; Shu, C.; Zhong, M.; Fan, X.; Yu, Z.; Huang, W.; Yan, D. Irradiation tolerance of an optically transparent polyimide film under 1 MeV electron beam. *Appl. Surf. Sci.* **2022**, *583*, 152558.
3 Lei, Y.; Zhang, L.; Zhou, L.; Yu, J.; Zhao, G.; Guo, L.; Zhang, D.; Qi, H. Proton irradiation-induced changes in the tribological performance of polyimide composites. *Tribol. Int.* **2022**, *167*, 107427.
4 Cherkashina, N.; Pavlenko, V.; Noskov, A. Synthesis and property evaluations of highly filled polyimide composites under thermal cycling conditions from −190 °C to +200 °C. *Cryogenics (Guildf)* **2019**, *104*, 102995.
5 De Oliveira, P. R.; Sukumaran, A. K.; Benedetti, L.; John, D.; Stephens, K.; Chu, S. H.; Park, C.; Agarwal, A. Novel polyimide-hexagonal boron nitride nanocomposites for synergistic improvement in tribological and radiation shielding properties. *Tribol. Int.* **2023**, *189*, 108936.
6 Kim, S. D.; Lee, B.; Byun, T.; Chung, I. S.; Park, J.; Shin, I.; Ahn, N. Y.; Seo, M.; Lee, Y.; Kim, Y. Poly(amide-imide) materials for transparent and flexible displays. *Sci. Adv*. **2018,** *4*, eaau1956.
7 Xu, Z.; Li, M.; Xu, M.; Zou, J.; Tao, H.; Wang, L.; Peng, J. Light extraction of flexible OLEDs based on transparent polyimide substrates with 3-D photonic structure. *Org. Electron.* **2017**, *44*, 225–231,
8 Park, C. I.; Seong, M.; Kim, M. A.; Kim, D.; Jung, H.; Cho, M.; Lee, S. H.; Lee, H.; Min, S.; Kim, J.; others World's first large size 77-inch transparent flexible OLED display. *J. Soc. Inf. Disp*. **2018,** *26*, 287–295.
9 Ke, T. Y.; Kang, T.; Lee, C. T.; Chen, C. Y.; Su, W. J.; Wang, W. T.; Huang, Z. S.; Wang, J. C.; Hsu, S. T.; Wang, C. L.; others Flexible OLED display with 620 °C LTPS TFT and touch sensor manufactured by weak bonding method. *J. Soc. Inf. Disp*. **2020,** *28*, 392–400.
10 Zhang, M.; Wang, L.; Xu, H.; Song, Y.; He, X. Polyimides as promising materials for lithiumion batteries: a review. *Nanomicro Lett.* **2023**, *15*, 135.
11 Li, M.; Sheng, L.; Xu, R.; Yang, Y.; Bai, Y.; Song, S.; Liu, G.; Wang, T.; Huang, X.; He, J. Enhanced the mechanical strength of polyimide (PI) nanofiber separator via PAALi binder for lithium ion battery. *Compos. Commun.* **2021**, *24*, 100607.
12 Huang, X.-W.; Liao, S.-Y.; Liu, Y.-D.; Rao, Q.-S.; Peng, X.-K.; Min, Y.-G. Design, fabrication and application of PEO/CMC-Li@ PI hybrid polymer electrolyte membrane in all-solid-state lithium battery. *Electrochimica* **2021**, *389*, 138747.
13 Parsaei, S.; Zebarjad, S. M.; Moghim, M. H. Fabrication and post-processing of PI/PVDF- HFP/PI electrospun sandwich separators for lithium-ion batteries. *Polym. Eng. Sci.* **2022**, *62*, 3641–3651.
14 Eixeres, B.; Sanchez-Caballero, S.; Peydro, M.; Parres, F.; Selles, M. Influence of injection molding process conditions on the mechanical properties of CF-PPS/PTFE composites. *Alex. Eng. J.* **2025**, *123*, 381–391.
15 Xu, H.; Gong, L. X.; Wang, X.; Zhao, L.; Pei, Y. B.; Wang, G.; Liu, Y. J.; Wu, L. B.; Jiang, J. X.; Tang, L. C. Influence of processing conditions on dispersion, electrical and mechanical properties of graphene-filled-silicone rubber composites. *Compos. Part A Appl. Sci. Manuf.* **2016**, *91*, 53–64.
16 Yang, C.; Tian, X.; Li, D.; Cao, Y.; Zhao, F.; Shi, C. Influence of thermal processing conditions in 3D printing on the crystallinity and mechanical properties of PEEK material. *J. Mater. Process. Technol.* **2017**, *248*, 1–7.
17 Vanheusden, C.; Samyn, P.; Goderis, B.; Hamid, M.; Reddy, N.;

Graphical Abstract

Processing-integrated Machine Learning Models for Predicting and Optimizing Mechanical Properties of Polyimides

Wei-Long Hu, Hao-Ke Qiu, En-Zhe Jing, Wan-Chen Zhao, Hai-Yang Huo, and Zhao-Yan Sun

University of Science and Technology of China; Changchun Institute of Applied Chemistry, Chinese Academy of Sciences; Jilin Provincial International Cooperation Key Laboratory for Polymer Processing Physics

A machine-learning framework was developed that integrates molecular structures and processing conditions to predict and optimize the mechanical properties of polyimides. The model identifies key structure-processing-property relationships and enables automated prediction of optimal processing conditions from a SMILES string and a user-defined number of optimization iterations inputs.

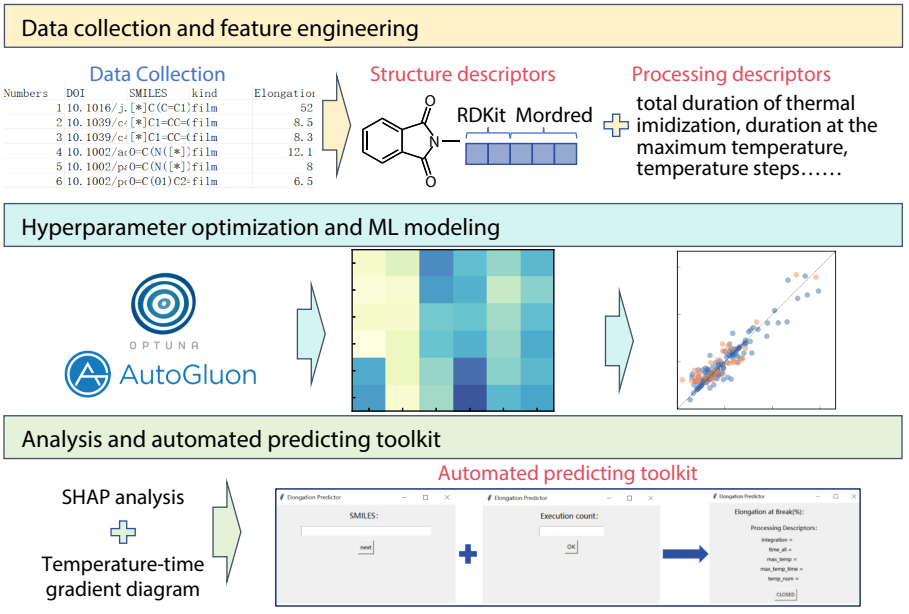

Chinese J. Polym. Sci., 2026 *https://doi.org/10.1007/s10118-026-3643-4*

Ethirajan, A.; Peeters, R.; Buntinx, M. Extrusion and injection molding of poly(3-hydroxybutyrate-co-3- hydroxyhexanoate) (PHBHHx): influence of processing conditions on mechanical properties and microstructure. *Polymers* **2021**, *13*, 4012.

18 Li, J.; Zhang, H.; Chen, J. Z. Structural prediction and inverse design by a strongly correlated neural network. *Phys. Rev. Lett.* **2019**, *123*, 108002.

19 Zhao, H.; Duan, P.; Li, Z.; Chen, Q.; Yue, T.; Zhang, L.; Ganesan, V.; Liu, J. Unveiling the multiscale dynamics of polymer vitrimers via molecular dynamics simulations. *Macromolecules* **2023**, *56*, 9336–9349.

20 Gao, L.; Lin, J.; Wang, L.; Du, L. Machine learning-assisted design of advanced polymeric materials. *Acc. Mater. Res.* **2024**, *5*, 571–584.

21 Zhang, K.; Gong, X.; Jiang, Y. Machine learning in soft matter: from simulations to experiments. *Adv. Funct. Mater*. **2024,** 2315177.

22 Liu, L.; Li, Y.; Zheng, J.; Li, H. Expert-augmented machine learning to accelerate the discovery of copolymers for anion exchange membrane. *J. Membr. Sci.* **2024**, *693*, 122327.

23 Dong, Q.; Xu, Z.; Song, Q.; Qiang, Y.; Cao, Y.; Li, W. Automated search strategy for novel ordered structures of block copolymers. *ACS Macro Lett.* **2024,** *13*, 987–993.

24 Qiu, H.; Sun, Z. Y. On-demand reverse design of polymers with PolyTAO. *Npj Comput. Mater.* **2024**, *10*, 273.

25 Lu, R.; Han, Y.; Hu, J.; Xu, D.; Zhong, Z.; Zhou, H.; Zhao, T.; Jiang, J. Deep learning model for precise prediction and design of low-melting point phthalonitrile monomers. *Chem. Eng. J.* **2024**, *497*, 154815.

26 Qiu, H.; Zhao, W.; Pei, H.; Li, J.; Sun, Z.-Y. Highly accurate prediction of viscosity of epoxy resin and diluent at various temperatures utilizing machine learning. *Polymer* **2022**, *256*, 125216.

27 Jumper, J.; Evans, R.; Pritzel, A.; Green, T.; Figurnov, M.; Ronneberger, O.; Tunyasuvu- nakool, K.; Bates, R.; Žídek, A.; Potapenko, A. Highly accurate protein structure prediction with AlphaFold. *Nature* **2021**, *596*, 583–589.

28 Xu, Y.; Liu, X.; Cao, X.; Huang, C.; Liu, E.; Qian, S.; Liu, X.; Wu, Y.; Dong, F.; Qiu, C.-W. Artificial intelligence: A powerful paradigm for scientific research. *Innovation* **2021,** *2*, 4

29 Qiu, H.; Liu, L.; Qiu, X.; Dai, X.; Ji, X.; Sun, Z.-Y. PolyNC: a natural and chemical language model for the prediction of unified polymer properties. *Chem. Sci.* **2024**, *15*, 534−544.

30 Gao, H.; Struble, T. J.; Coley, C. W.; Wang, Y.; Green, W. H.; Jensen, K. F. Using machine learning to predict suitable conditions for organic reactions. *ACS Cent. Sci.* **2018**, *4*, 1465−1476.

31 Mannodi-Kanakkithodi, A.; Chandrasekaran, A.; Kim, C.; Huan, T. D.; Pilania, G.; Botu, V.; Ramprasad, R. Scoping the polymer genome: a roadmap for rational polymer dielectrics design and beyond. *Mater. Today* **2018**, *21*, 785−796.

32 Zhang, S.; He, X.; Xia, X.; Xiao, P.; Wu, Q.; Zheng, F.; Lu, Q. Machine-learning-enabled framework in engineering plastics discovery: a case study of designing polyimides with desired glass-transition temperature. *ACS Appl. Mater. Interfaces* **2023**, *15*, 37893−37902.

33 Uddin, M. J.; Fan, J. Interpretable machine learning framework to predict the glass transition temperature of polymers. *Polymers* **2024**, *16*, 1049.

34 Qiu, H.; Qiu, X.; Dai, X.; Sun, Z. Y. Design of polyimides with targeted glass transition temperature using a graph neural network. *J. Mater. Chem. C* **2023**, *11*, 2930−2940.

35 Dong, X.; Wan, B.; Zheng, M.S.; Huang, L.; Feng, Y.; Yao, R.; Gao, J.; Zhao, Q. L.; Zha, J. W. Dual-effect coupling for superior dielectric and thermal conductivity of polyimide composite films featuring "crystal-like phase" structure. *Adv. Mater.* **2024**, *36*, 2307804.

36 Yang, H. L.; Liu, D. G.; Duan, K.; Wang, Y.; Qiu, H.; Zhang, J.; Fu, Y.; Sun, Z. Y. Machine learning-guided design of bio-based furan-containing polyimides with tunable dielectric properties. *Macromolecules* **2025**, *58*, 9031−9043.

37 Luo, G.; Huan, F.; Sun, Y.; Shi, F.; Deng, S.; Wang, J.G. Machine learning-based high-throughput screening for high-stability polyimides. *Ind. Eng. Chem. Res.* **2024**, *63*, 21110−21122.

38 Zhang, S.; He, X.; Xiao, P.; Xia, X.; Zheng, F.; Xiang, S.; Lu, Q. Interpretable machine learning for investigating the molecular mechanisms governing the transparency of colorless transparent polyimide for OLED cover windows. *Adv. Funct. Mater.* **2024**, *34*, 2409143.

39 Yue, T.; He, J.; Tao, L.; Li, Y. High-throughput screening and prediction of high modulus of resilience polymers using explainable machine learning. *J. Chem. Theory Comput.* **2023**, *19*, 4641−4653.

40 Tao, L.; He, J.; Munyaneza, N. E.; Varshney, V.; Chen, W.; Liu, G.; Li, Y. Discovery of multi-functional polyimides through high-throughput screening using explainable machine learning. *Chem. Eng. J.* **2023**, *465*, 142949.

41 Lei, H.; Qi, S.; Wu, D. Hierarchical multiscale analysis of polyimide films by molecular dynamics simulation: Investigation of thermo-mechanical properties. *Polymer* **2019**, *179*, 121645.

42 Hu, W.; Jing, E.; Qiu, H.; Sun, Z. Y. Discovering polyimides and their composites with targeted mechanical properties through explainable machine learning. *J. Mater. Info.* **2025**, *5*, 1.

43 Chen, G.; Shen, Z.; Iyer, A.; Ghumman, U. F.; Tang, S.; Bi, J.; Chen, W.; Li, Y. Machine-learning-assisted de novo design of organic molecules and polymers: opportunities and challenges. *Polymers* **2020**, *12*, 163.

44 Campos, D.; Ji, H. IMG2SMI: translating molecular structure images to simplified molecular-input line-entry system. arXiv preprint arXiv:2109.04202 2021.

45 Tao, L.; Varshney, V.; Li, Y. Benchmarking machine learning models for polymer informatics: an example of glass transition temperature. *J. Chem. Inf. Model.* **2021**, *61*, 5395−5413.

46 Chen, G.; Tao, L.; Li, Y. Predicting polymers' glass transition temperature by a chemical language processing model. *Polymers* **2021**, *13*, 1898.

47 Wu, S.; Kondo, Y.; Kakimoto, M.-a.; Yang, B.; Yamada, H.; Kuwajima, I.; Lambard, G.; Hongo, K.; Xu, Y.; Shiomi, J.; others Machine-learning-assisted discovery of polymers with high thermal conductivity using a molecular design algorithm. *Npj Comput. Mater.* **2019,** *5*, 66.

48 Zhang, Y.; Xu, X. Machine learning glass transition temperature of polyacrylamides using quantum chemical descriptors. *Polym. Chem.* **2021**, *12*, 843−851.

49 Liu, L.; Chen, W.; Liu, T.; Kong, X.; Zheng, J.; Li, Y. Rational design of hydrocarbon-based sulfonated copolymers for proton exchange membranes. *J. Mater. Chem. A* **2019**, *7*, 11847-11857.

50 Xiao, X.; Zou, Y.; Huang, J.; Luo, X.; Yang, L.; Li, M.; Yang, P.; Ji, X.; Li, Y. An interpretable model for landslide susceptibility assessment based on Optuna hyperparameter optimization and Random Forest. *Geomat. Nat. Haz. Risk.* **2024**, *15*, 2347421.